

Synchrotron Spectromicroscopy for the Life Sciences: General Considerations and Special Procedures

G. Margaritondo,¹ Gelsomina De Stasio^{1,2}

¹ Institut de Physique Appliquée, Ecole Polytechnique Fédérale, CH-1015 Lausanne, Switzerland

² Istituto di Struttura della Materia del CNR, I-00044 Frascati, Italy

Received 30 July 1996; revised 19 November 1996

ABSTRACT: The effort to apply synchrotron spectromicroscopy techniques to life science problems is definitely beyond the feasibility-test stage. Furthermore, the commissioning of ultrabright, third-generation soft-X-ray sources such as Elettra in Trieste or the advanced light source in Berkeley has boosted this effort, most notably in the areas of scanning and electron-imaging photoelectron spectromicroscopy. Besides producing research results, the effort also develops new procedures and finds solutions for new conceptual problems. We first briefly review the basic experimental techniques in this domain; then we discuss some specific experimental issues, such as the specimen preparation problems caused by peculiar features of the techniques, e.g., their surface sensitivity. Third, we briefly present conceptual considerations on the optimization of the data-taking procedures. Finally, we illustrate the applications in biology with a few specific research examples, and analyze the probable future developments in this area. © 1997 John Wiley & Sons, Inc. *Int J Imaging Syst Technol*, **8**, 188–203, 1997

I. INTRODUCTION: ELECTRON MICROSCOPY WITH INTERNAL ELECTRONS

Electron microscopy has been for decades one of the basic techniques in biological and medical research. All types of electron microscopy approaches are based on the interaction of the specimen with a beam of electrons; this primary beam is typically generated by an electron gun. Photoelectron spectromicroscopy [1–6] is a notable exception, since the electrons are generated from inside the specimen by means of the photoelectric effect.

This well-known effect is the ejection of electrons from a system illuminated with ultraviolet or X-ray light. Its basic theory was developed [7] by Albert Einstein in 1905: light of frequency ν behaves as if it was formed by energy quanta $h\nu$ —the photons.

A photon absorbed by a system can transfer its energy to one of its electrons, enabling it to overcome the binding energy barrier and to be ejected, becoming a “photoelectron.”

The effect is extensively used as a fine and powerful chemical probe [7]. Consider, for example, the ejection of a “core” electron which is strongly bound to one of the atoms of the system. The ejected electron carries information on the atom: specifically, on the corresponding chemical elements and on its chemical status, i.e., on its chemical bonds. Figure 1 provides a very simplified picture of how this information can be extracted. This powerful approach to chemical analysis has been extensively used for decades [7] under the general name of “photoelectron spectroscopy” and more specific acronyms such as ESCA (electron spectroscopy for chemical analysis).

Why, then, should one not combine photoelectron spectroscopy with electron microscopy and perform the analysis on a microscopic scale? The answer, until quite recently, was that no photon source existed to obtain the required photon flux and brightness. This situation, however, radically changed with the advent of sophisticated synchrotron light sources [1–6,8].

The microscopic-scale version of photoelectron spectroscopy—known as photoelectron spectromicroscopy—was discovered in the late 1980s [1–6]. In a few years, it has emerged as one of the most powerful experimental techniques for materials science. Furthermore, the achievement of spatial resolution better than the typical size of cells has made the same approach suitable for biological and medical research [2].

We present a short overview of this novel approach, with special emphasis on biological applications [2]. First, we briefly review different approaches to photoelectron spectromicroscopy, in the two general classes of scanning and imaging spectromicroscopy [1–6]. Then, we discuss specific problems concerning the applications to biological specimens. Before reviewing specific examples of applications, we present a short discussion of the data-taking strategies and of the optimization of the information content [9].

The examples include data taken with the imaging spectromicroscopes X-ray secondary electron-emission microscope

Correspondence to: G. Margaritondo

Contract grant sponsor: Fonds National Suisse de la Recherche Scientifique

Contract grant sponsor: European Community

Contract grant sponsor: US Office of Naval Research

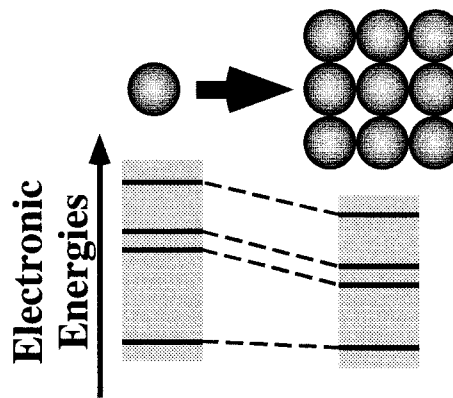
Contract grant sponsor: US National Science Foundation

Contract grant sponsor: US Department of Energy

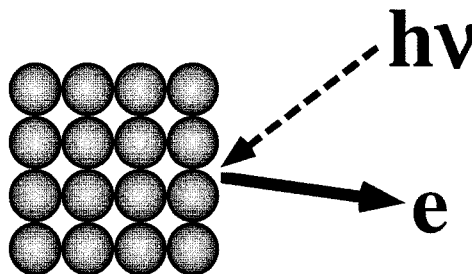
Contract grant sponsor: Ecole Polytechnique Fédérale de Lausanne

Contract grant sponsor: Sincrotrone Trieste SCpA

(a) Formation of chemical bonds



(b) Photoelectric effect



The photoelectric effect increases the electron energies (c) by $h\nu$ before ejection into the vacuum (d)

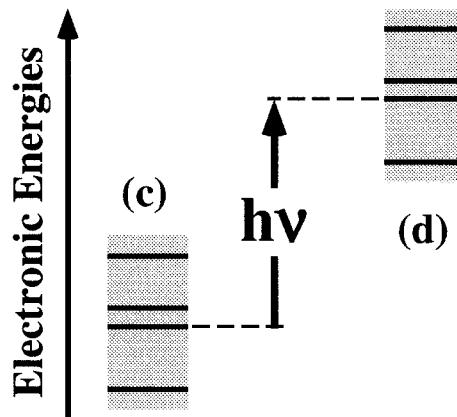


Figure 1. Simplified picture of photoemission-based techniques. Besides forming a solid, atoms contain electrons which occupy specific energy levels. After the formation of chemical bonds, the energy levels are modified. When an electron absorbs a photon of energy $h\nu$ and becomes a photoelectron, its energy equals that of the initial state plus $h\nu$. Thus, by measuring the photoelectron energy one can retrieve the initial energy and information on the chemical bonds that influence it. Similarly, information on the chemical bonds can be retrieved from other photoelectron properties, such as the direction of ejection.

(XSEM) [10,11]—including its transmission microscopy version [12]—and microscope à émission de photoélectrons par illumination synchrotronique de type onduleur (MEPHISTO) (photoelectron emission microscope by synchrotron undulator illumination) (G. De Stasio et al., unpublished), and with the scanning spectromicroscope ESCA microscopy (M. Kiskinova, unpublished; L. Casalio, L. Gregoratti, M. Gunter, A. Kolmakov, L. Kovac, M. Marsi, and M. Kiskinova, private communication; A. Kolmakov, L. Kovac, M. Günther, L. Casalis, L. Gregoratti, M. Marsi, and M. Kiskinova, unpublished). Finally, we analyze the probable evolution of this domain, considering the recent

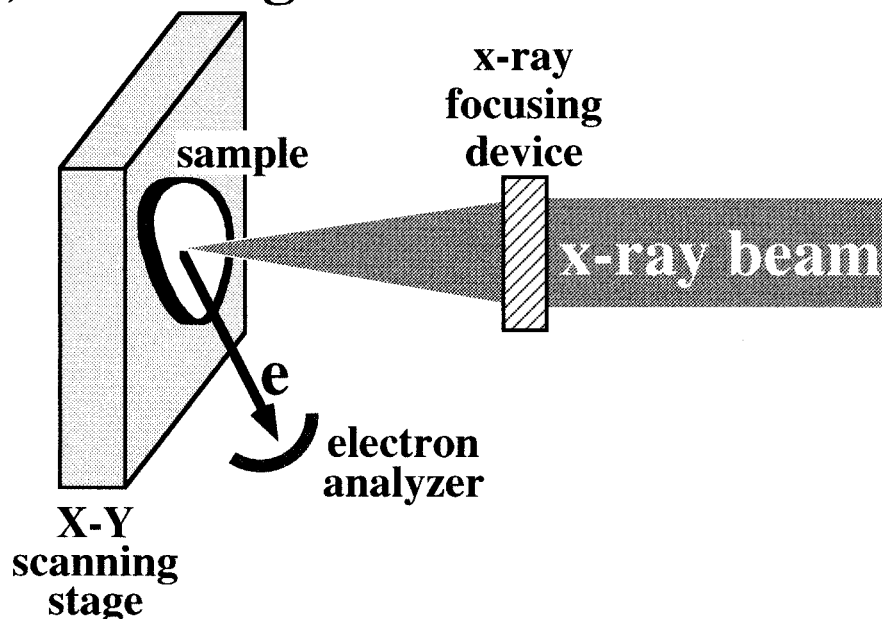
commissioning of third-generation synchrotron sources and the first proposals for fourth-generation facilities [13].

II. AN OVERVIEW OF PHOTOELECTRON SPECTROMICROSCOPY TECHNIQUES

Spectromicroscopy techniques [1–6] fall into the two general classes schematically illustrated in Figure 2. In the case of scanning spectromicroscopy, high lateral resolution is achieved by focusing the monochromatized X-ray beam with a special device. Imaging spectromicroscopy obtains the lateral resolution by processing the ejected photoelectrons with an electron optics system.

The two modes of photoemission spectromicroscopy:

(a) scanning:



(b) electron imaging:

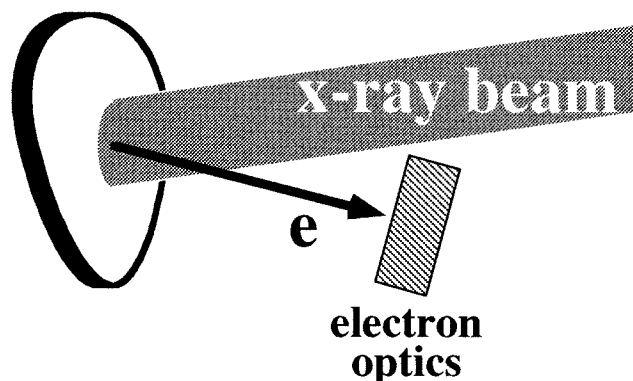


Figure 2. Scheme of the two classes of photoemission spectromicroscopy techniques [1–6]. (Top) Scanning mode: One focuses the photon beam into a small area. Then, photoelectron spectra can be obtained from that microscopic area. Alternatively, one can fix the energy of detected photoelectrons and scan the sample with respect to the focused photon beam, obtaining two-dimensional photoelectron-intensity microimages. (Bottom) Imaging mode: The fixed-energy photons flood the sample and the photoelectrons are processed by an electron optics system. One thus obtains photoelectron intensity microimages without selecting the photoelectron energy: The chemical information is extracted by controlling the photon energy. One can also take spectra in this mode from selected microareas by measuring the photoelectron emission intensity as a function of the photon energy; these spectra reflect the local X-ray absorption coefficient [14].

We first analyze imaging spectromicroscopy: The microimage contrast reflects the photoelectron yield fluctuations over the emitting surface. “White” corresponds to areas with strong photoelectron emission, and “black” to areas with little or no emission.

In turn, fluctuations in the photoelectron intensity are caused [1–6] by two factors: microscopic chemical differences and the microscopic surface geometry. We will concentrate our attention on the chemical contrast, but one should always keep in mind

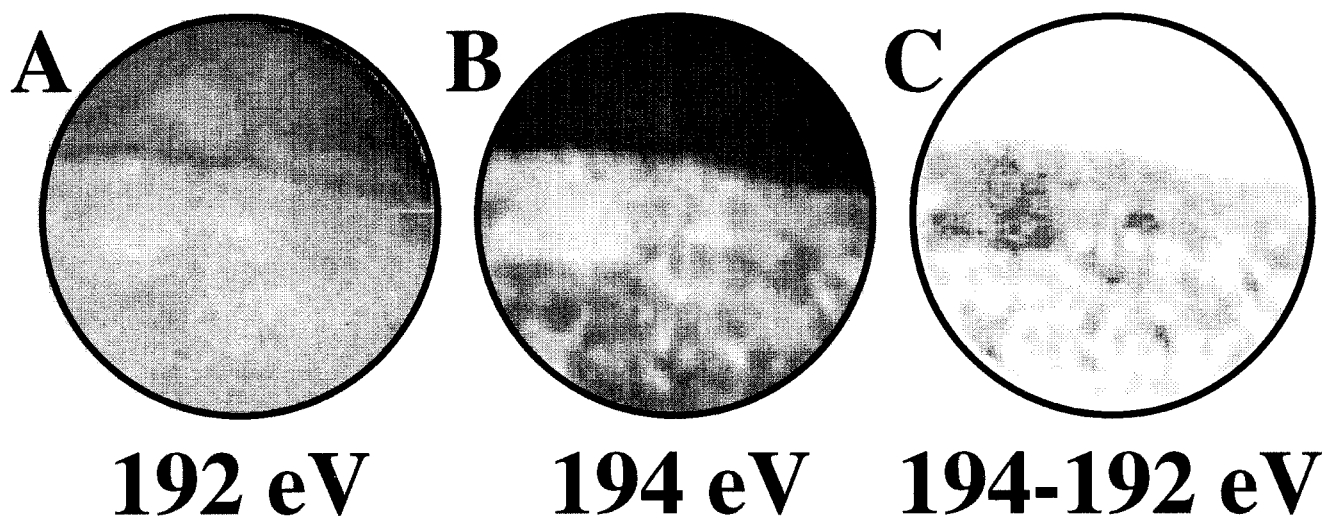


Figure 3. (A) XSEM [10] micrograph taken on a silicon substrate (top) partly covered by a dried droplet (below) of a sodium tetraborate solution. The image was acquired at 192 eV photon energy, below the B1s absorption edge. (B) Identical image acquired at 194 eV. (C) Digital subtraction of the image at 192 eV from the image at 194 eV, revealing the microscopic distribution map of boron.

the possible effects of geometry while extracting information from the data.

What is the origin of the chemical contrast? Consider the two images (G. De Stasio, unpublished) on the left-hand side and center of Figure 3, taken on a silicon substrate partly covered by a dried droplet of a boron-compound (sodium tetraborate) solution. The images were obtained with two different photon energies, $h\nu = 192$ and 194 eV, right below and right above the X-ray spectral absorption edge of boron. Thus, the boron-containing part of the surface absorbs more X-rays in the second than in the first image. In turn, more X-ray absorption means more emission of photoelectrons: thus, the boron-containing area appears brighter in the second image than in the first. This chemical contrast can be enhanced by digital pixel-by-pixel subtraction of the two images, whose result is shown on the right hand side of Figure 3. The difference image provides a clear microscopic distribution map of boron.

More detailed spectral information can be extracted for selected small areas with the following technique. The emitted photoelectron intensity from each microarea is detected as a function of the photon energy: This plot reflects [14] the local X-ray absorption coefficient. The appearance of an X-ray absorption edge immediately reveals that the corresponding chemical element is present in the microarea. Furthermore, the edge lineshape reflects the chemical state of the element and its nearest-neighbor atomic coordination [15].

We now turn our attention to scanning spectromicroscopy. Since the photon beam is strongly focused, the photoelectrons are emitted from a small area. By studying their properties, one can derive those of the small area. For example, Figure 1 indicates how, by detecting the photoelectron energy, one can measure the energies of the electronic states, and from these identify the elements that are present in the microarea and their chemical status.

Furthermore, one can produce photoelectron intensity micro-images by scanning the position of the sample with respect to the focused photon beam. The basic difference between the mi-

croimages produced by imaging and scanning spectromicroscopy is that in the second case only photoelectrons of a selected kinetic energy are detected. As one can see in Figure 1, a given photoelectron kinetic energy corresponds to a given energy level of a given element. Thus, the scanning photoelectron micrographs reflect once again the distribution of chemical elements over the sample surface—but, contrary to imaging spectromicroscopy, the chemical information is obtained by selecting the photoelectron energy rather than by comparing images taken at different photon energies.

Each class of spectromicroscopy techniques presents advantages and disadvantages; one should select the best approach depending on the system to be investigated and on the properties that one wants to derive. In general, imaging techniques are better than scanning techniques for the study of biological specimens [2], whereas the opposite is true in the study of energy barriers at interfaces [16,17].

Imaging spectromicroscopy is preferable for biological applications, from several different points of view [2]. First of all, it takes all points of an image simultaneously; thus, the overall image taking time is much reduced with respect to scanning spectromicroscopy—and this is quite important in biology experiments that require surveying large specimen areas. Second, its chemical analysis based on scanning the photon energy is not only powerful but also quite fast—and this is again a crucial factor in analyzing large areas. Note that modifying the photon energy is difficult or impossible for scanning spectromicroscopy: Commonly used lenses for photon focusing [1–6] are photon energy bandpass devices, thus incompatible with wide-band modifications of the photon energy.

III. SOME EXAMPLES OF SPECTROMICROSCOPY INSTRUMENTS

A. Scanning Spectromicroscopes: From MAXIMUM to ESCA Microscopy. Several scanning spectromicroscopes have been implemented in recent years, based on different types of photon focusing devices. The two most popular devices are the

MAXIMUM

(Multiple-Application X-ray Imaging Undulator Microscope)

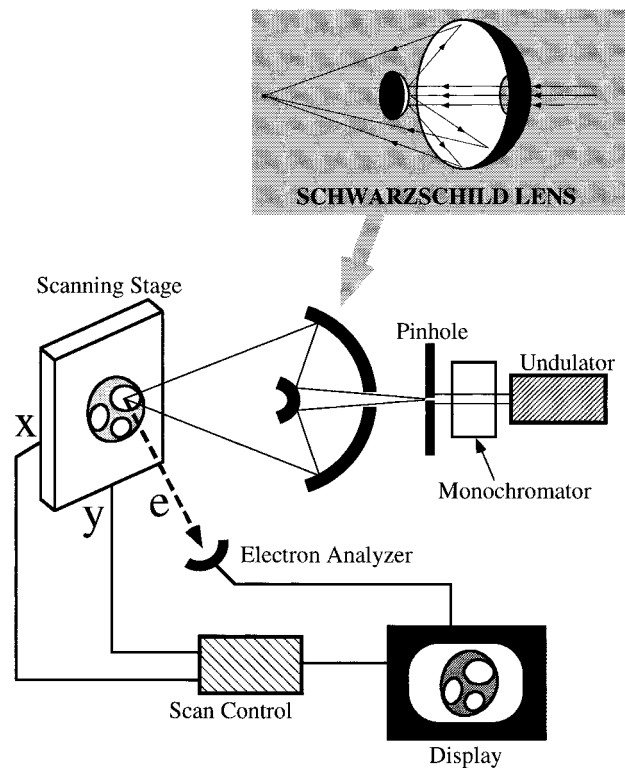


Figure 4. Artist's view of the scanning spectromicroscope MAXIMUM (Refs. 1, 18, 19, and 23).

Schwarzschild objective [1,18] and the Fresnel zone plates [13,20,21]. The first one is a combination of a concave and a convex mirror, both enabled to work at near-normal reflection by multilayer coatings—which, however, are photon energy band-pass devices.

The Schwarzschild objective is the core of the MAXIMUM [1,18] and SuperMAXIMUM [22] spectromicroscopes, the first initially commissioned at the Wisconsin Synchrotron Radiation Center and then moved to the advanced light source (ALS), and the second soon to be commissioned on Elettra. Figure 4 shows an artist's view of MAXIMUM, in which the basic features of a scanning spectromicroscope are easily recognizable.

After its original use as the first scanning spectromicroscope [1,23], MAXIMUM reached a lateral resolution beyond $0.1 \mu\text{m}$ [18] and was used for a variety of experiments. Most of these concerned solid–solid interfaces, but the instrument was also used for some of the early experiments in biological spectromicroscopy. Specifically, it produced the first photoelectron micrographs of brain cell systems [24].

The Fresnel zone plate used for scanning spectromicroscopy [13,20,21], on the other hand, is the X-ray counterpart of the very popular devices used for visible light. The focusing action is based on a series of concentric circular transmitting and absorbing zones of decreasing size. The total diameter of the device is determined by the minimum zone size that one can fabricate,

typically with electron beam lithography. The best devices [20,21] have outer zones with a size of a few hundred angstroms; even so, the total diameter does not exceed a fraction of a millimeter, which creates some difficulty in practical use.

The best performing Fresnel zone plate photoelectron spectromicroscope so far is the ESCA microscopy beamline of Elettra (M. Kiskinova, unpublished; L. Casalis, L. Gregoratti, M. Gunter, A. Kolmakov, L. Kovac, M. Marsi, and M. Kiskinova, private communication; A. Kolmakov, L. Kovac, M. Günther, L. Casalis, L. Gregoratti, M. Marsi, and M. Kiskinova, unpublished). Its top performances are a lateral resolution of $0.1 \mu\text{m}$ and a photoelectron energy resolution of 500 meV. With this device, Kiskinova and co-workers (M. Kiskinova, unpublished; L. Casalis, L. Gregoratti, M. Gunter, A. Kolmakov, L. Kovac, M. Marsi, and M. Kiskinova, private communication; A. Kolmakov, L. Kovac, M. Günther, L. Casalis, L. Gregoratti, M. Marsi, and M. Kiskinova, unpublished), in cooperation with many external groups, have been able to perform fine chemical analysis of very complicated specimens. One example [25,26] is shown in Figure 5: We see three different scanning photoelectron micrographs of the same specimen, consisting of an Ag-covered Si substrate with a gold overlayer. The photoelectron energies of the micrographs correspond to core level energies of Si, Ag, and Au.

The different contrast in the different features reflects the microscopic distribution of the corresponding elements, as well as

Si 2p

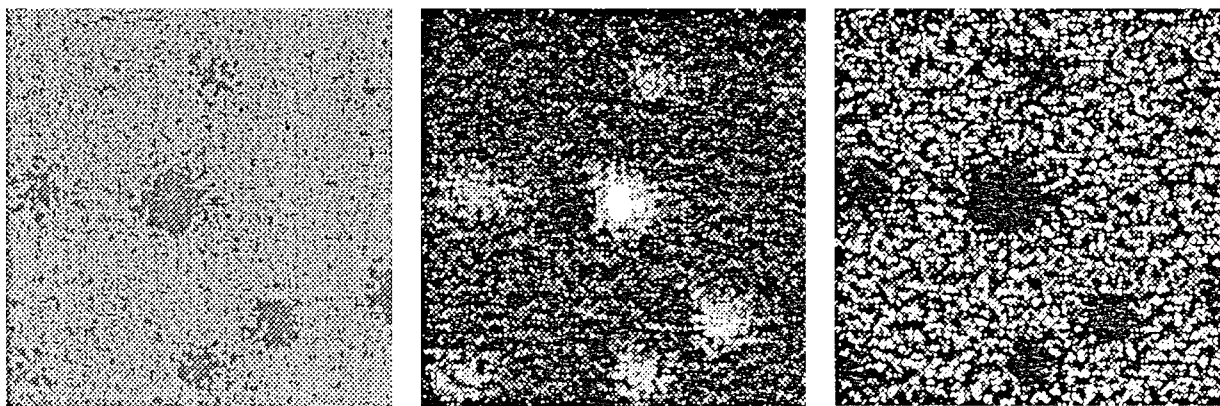
Au 4f_{7/2}Ag 3d_{5/2}

Figure 5. Photoelectron micrographs showing the lateral distribution of Si, Au, and Ag for an Ag-covered Si(111) + Au substrate. The system includes two-dimensional (2D) and three-dimensional (3D) phases. Data from the ELETTRA ESCA microscopy beamline (M. Kiskinova, unpublished; L. Casalis, L. Gregoratti, M. Gunter, A. Kolmakov, L. Kovac, M. Marsi, and M. Kiskinova, private communication; A. Kolmakov, L. Kovac, M. Günther, L. Casalis, L. Gregoratti, M. Marsi, and M. Kiskinova, unpublished).

geometric features. Specifically, we can see both two-dimensional phase and smaller, clusterlike, three-dimensional features. A fine spectroscopic analysis (M. Kiskinova, unpublished; L. Casalis, L. Gregoratti, M. Gunter, A. Kolmakov, L. Kovac, M. Marsi, and M. Kiskinova, private communication; A. Kolmakov, L. Kovac, M. Günther, L. Casalis, L. Gregoratti, M. Marsi, and M. Kiskinova, unpublished) demonstrated that reacted gold is present in both phases, whereas metallic gold is present only in the three-dimensional phase. This is very valuable information in assessing the causes of the chemical reactivity for this type of system.

B. Imaging Spectromicroscopes: From the XSEM to MEPHISTO. X-ray secondary electron-emission microscopy, developed by Tonner and co-workers [10] at the University of Wisconsin, was the first instrument in this class. MEPHISTO (G. De Stasio et al., unpublished) is its natural evolution toward higher lateral resolution and a better correction of the aberrations in the image produced by the electron optical system.

Figure 6 shows an artist's view of MEPHISTO. The basic philosophy is still quite similar to that of the XSEM or photoelectron emission microscope (PEEM) (STAIB, Germany). In MEPHISTO, a photon beam reaches the sample, which is negatively biased with respect to ground. Under X-ray illumination, the sample emits electrons which are accelerated (because of the negative sample bias) toward the system of electrostatic lenses which constitute the electron optics.

Each lens magnifies the photoelectron image. The overall magnified image produced by the electron optics is intensified by a microchannel plate device, then converted to a visible image by a phosphorous screen. A video acquisition system is used to monitor the visible image in real time and to take and store digitalized black-and-white individual pictures.

Besides taking microimages, the system can measure spectral curves (photoelectron intensity vs. photon energy) from selected image areas. As we have already seen, these are equivalent to X-ray spectral absorption curves [14].

Systems prior to MEPHISTO could achieve a maximum lateral resolution of the order of $0.5 \mu\text{m}$, and a partial correction for the image aberrations. Significant improvements have been introduced for MEPHISTO to go beyond these performance levels.

Specifically (G. De Stasio et al., unpublished), the number of optical elements and the maximum accelerating voltage have been increased. The design lateral resolution of a few hundred angstroms should bring MEPHISTO to the forefront of this class of instruments. The higher acceleration voltage also improves the reduction of chromatic aberrations.

The development of MEPHISTO began in 1995. The construction of its first version (with a preliminary electron optics system) initiated on October 18 of the same year, and the first images were delivered on November 20. Although not yet reaching the final design performances, this first version produced a large volume of real data. Quite recently, the implementation of the final optics system was completed and its commissioning stage initiated.

C. Imaging Spectromicroscopy in the Transmission Mode. An imaging spectromicroscope such as MEPHISTO can also be used as a transmission spectromicroscope [12]. X-rays transmitted through the investigated sample are converted into photoelectrons with a photocathode. The photoelectrons are then processed by the electron optical system producing submicron-resolution images.

Tests of this approach were performed [12] with the XSEM spectromicroscope on a specimen consisting of small Si features on an Si_3N_4 transmitting window. The images demonstrated excellent contrast due to the chemical difference between Si and Si_3N_4 . X-ray transmission vs. photon energy curves were also obtained for microscopic specimen areas.

This approach is closely related to contact X-ray microscopy using image-converter detectors. Early attempts can be traced to the work of Huang, who used a tungsten target as the X-ray source [27]. Polack and Lowenthal considered the effects of

MEPHISTO

Microscope à Emission de Photoélectrons par Illumination Synchrotronique de Type Onduleur

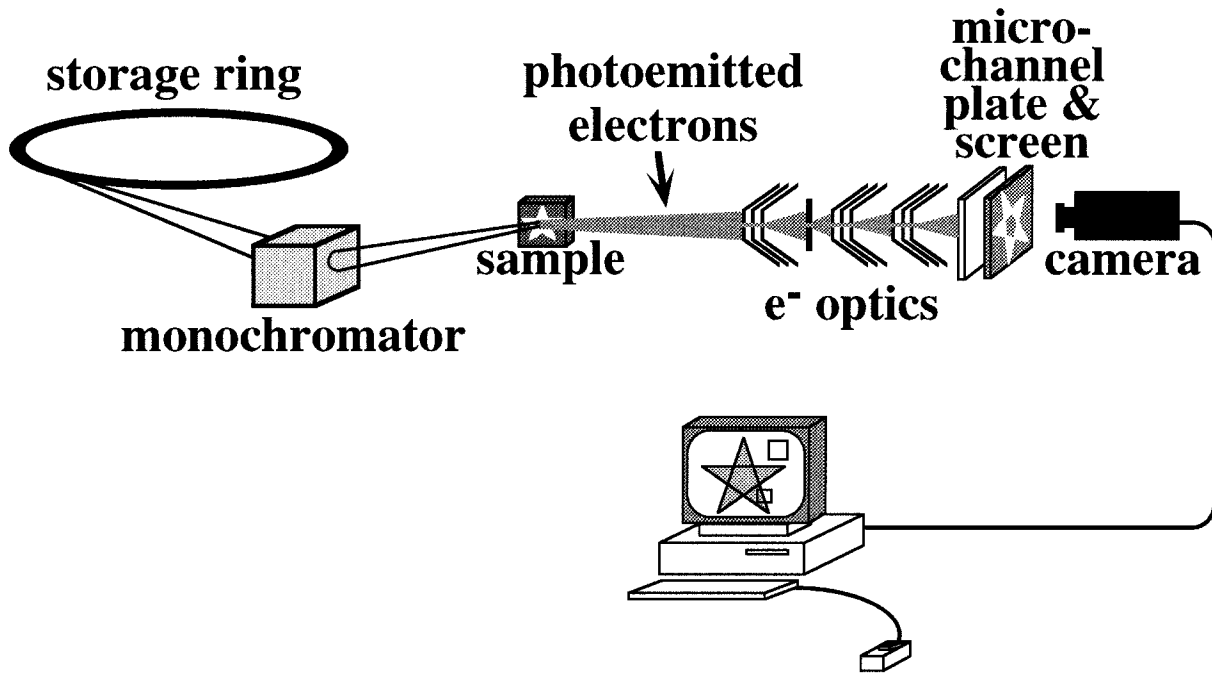


Figure 6. Artist's view of the MEPHISTO imaging spectromicroscope (G. De Stasio et al., unpublished).

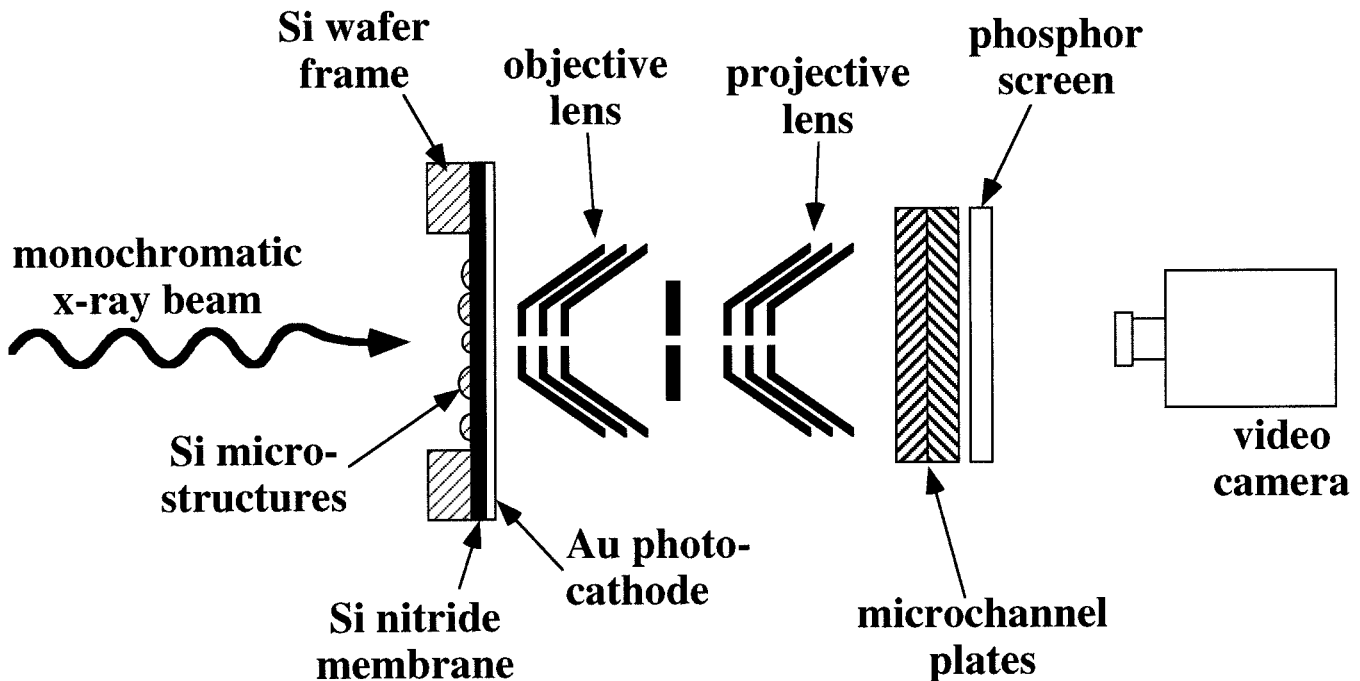


Figure 7. Scheme of the transmission spectromicroscopy apparatus of Ref. 12.

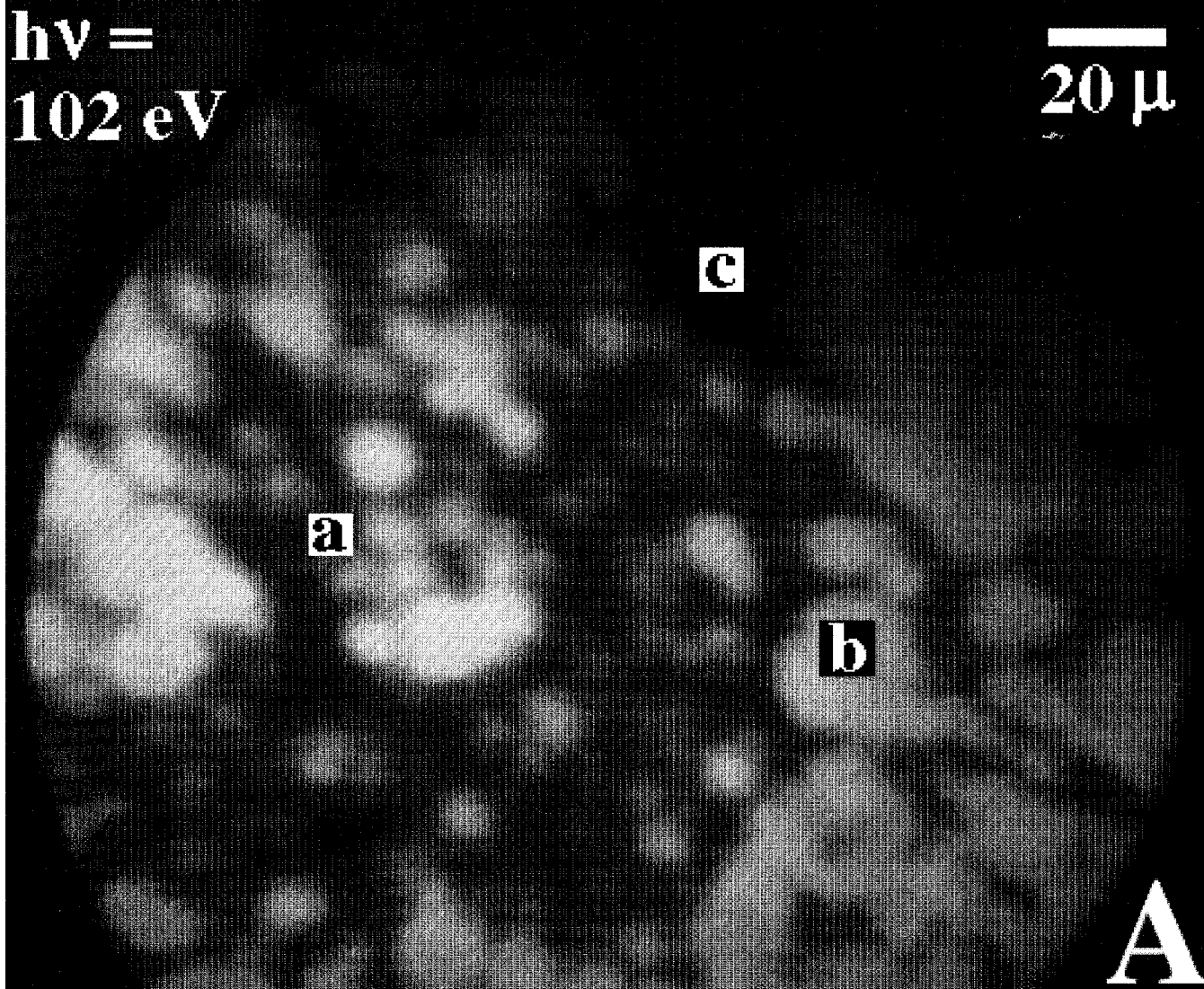


Figure 8. (A) Transmission micrograph of silicon microstructures (dark regions) on an Si_3N_4 membrane (lighter regions) obtained at a photon energy of 102 eV. (B) Transmission curves as a function of photon energy simultaneously taken in the areas labeled as a, b, and c in (A). Results from Ref. 12.

chromatic aberration as a limiting factor in the spatial resolution of transmission X-ray microscopy with an emission electron microscope as a detector [28]. They constructed an electromagnetic emission microscope with a Castaing–Henry energy filter, which was briefly used on the ACO synchrotron storage ring in Orsay.

Our approach reached better performances than any previous X-ray transmission photoelectron spectromicroscopy technique. Figure 7 shows the scheme [12] of the test apparatus. The X-ray beam was produced by the Aladdin storage ring at the Wisconsin Synchrotron Radiation Center, and monochromatized by a 6-m toroidal grating monochromator. Figure 8 refers to the first successful tests [12] which demonstrated the following performances: lateral resolution better than $0.5 \mu\text{m}$ and energy resolution (of the incident X-rays) of 0.1 eV.

In Figure 8(A), we can see silicon microstructures on the Si_3N_4 membrane. The photocathode consisted of a 50 Å evapo-

rated Au coating on the silicon nitride membrane. The photocathode coating was kept at a negative voltage bias of 4–8 kV and the first element of the XSEM objective lens was at ground. Besides taking images with the approach described above, we also took local intensity vs. photon energy spectra—which in this case are directly related to the photon intensity transmitted through the specimen.

The transmission micrograph of Figure 8(A), obtained at a photon energy of 102 eV, is a typical result of the first test. At 102 eV, silicon nitride is transparent, whereas the silicon microfeatures absorb photons, thus appearing as dark areas. The lateral resolution is better than $0.5 \mu\text{m}$.

Figure 8(B) demonstrates the spectromicroscopic capabilities of our approach. Transmission curves as a function of photon energy were simultaneously taken in the areas labeled as a, b, and c in Figure 8(A). All three curves exhibit features corre-

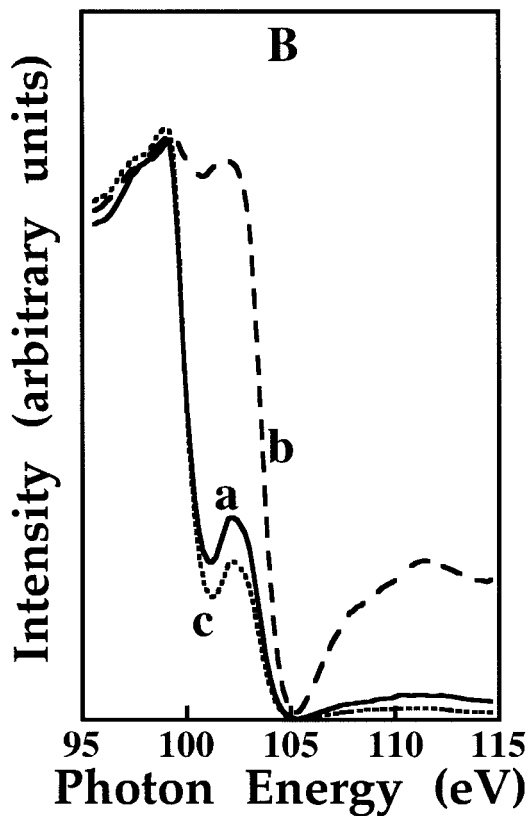


Figure 8. Continued

sponding to the silicon and silicon nitride Si2p absorption edges (100 and 104 eV). In curves a and c, which correspond to silicon microstructures in Figure 8(A), we see a strong silicon edge and a relatively weak silicon nitride edge. On the contrary, the silicon nitride edge is most prominent in curve b, which indeed corresponds to a bright area of Figure 8(A).

Note that no image processing was done on Figure 8(A). Even so, one can see a very high contrast despite the small sample thickness, which demonstrates the high sensitivity of the apparatus to chemical differences. This is of fundamental importance in specialized life-science applications such as the microchemical analysis of thin tissue sections.

IV. SPECIAL TECHNIQUES FOR BIOLOGICAL SPECIMEN HANDLING

Both scanning and imaging approaches require the experimental chamber to be under ultrahigh vacuum. Biological specimens therefore need to be fixed and dehydrated prior to the experiment. The fixation techniques [2] do not constitute a problem, since they had already been developed for conventional electron microscopy.

These fixation techniques, based on the exposure to chemicals such as paraformaldehyde and glutaraldehyde, guarantee that the chemical compounds of the specimen and their location are not altered during the dehydrating stage. This stability is obtained by crosslinking all the proteins that naturally constitute a cell or a tissue, and creating a mechanically rigid structure.

Besides ultrahigh vacuum, photoemission-based techniques

are affected by another potential problem: their high surface sensitivity [15]. For scanning techniques, surface sensitivity tends to be very high, since the inelastic-scattering mean free path of the electrons is of a few angstroms at the relevant kinetic energies. Note that one must consider the inelastic-scattering mean free path, since scanning spectromicroscopy analyzes primary photoelectrons which have not been inelastically scattered.

On the other hand, imaging spectromicroscopy detects photoelectrons without discriminating their energy. Therefore, the signal is dominated by low-energy electrons which are the product of multiple scattering. The escape depth for low-energy electrons is much longer [15] than for primary photoelectrons, and the probed depth reaches 100–500 Å.

Surface sensitivity nevertheless remains a potential problem for both types of spectromicroscopy in biological applications: One could end up probing only the outermost part of the specimen. Several remedies have been conceived to overcome this problem. Good results were obtained, for example, by decapping cells in a controlled way [29].

Another remedy is the incineration of the cells or the tissues [31]. This is obtained by exposing the specimens to a cold oxygen plasma which promotes the oxidation and volatilization of carbon, nitrogen, and hydrogen. The incineration strongly decreases the amount of material physically present in the sample, reducing its thickness and increasing the relative concentration of the remaining elements. The procedure does not cause element displacement; therefore, it does not alter the microscopic distribution of the elements, which is the subject of the investigation.

V. INFORMATION CONTENT AND OPTIMIZATION OF THE EXPERIMENTAL STRATEGIES

Before considering practical examples of photoelectron spectromicroscopy, we must discuss a rather delicate and often overlooked problem: the necessity of carefully planning the data-taking (and data analysis) strategy [9] to avoid unnecessary waste of expensive synchrotron radiation beamtime. This risk is a consequence of the transition from simple spectroscopy (or simple microscopy) to spectromicroscopy.

Spectroscopy is a one-dimensional technique which scans only one free variable such as the electron or photon energy; the result is an array of data points. Microscopy is a two-dimensional technique whose result is a two-dimensional matrix. Spectromicroscopy uses three free variables, and the ultimate result could be thought as a three-dimensional array. A small amount of wasted time per data point, therefore, is amplified much more dramatically than in spectroscopy or microscopy.

We can illustrate this point with a couple of examples. Suppose that you want to measure the spatial distribution of a given element, discriminating between two possible oxidation states. The information is sought by analyzing a given core level of that element; the energy position of the core level changes depending on the oxidation state. Thus, scanning micrographs taken at two different photoelectron energies reveal the spatial distribution of the two oxidation states.

How much energy resolution do you need to discriminate one oxidation state from the other? You must, of course, consider at the distance in energy between the two core-level positions. Typically, an energy resolution similar to this distance is sufficient.

Suppose instead that you overkill the problem by using 10

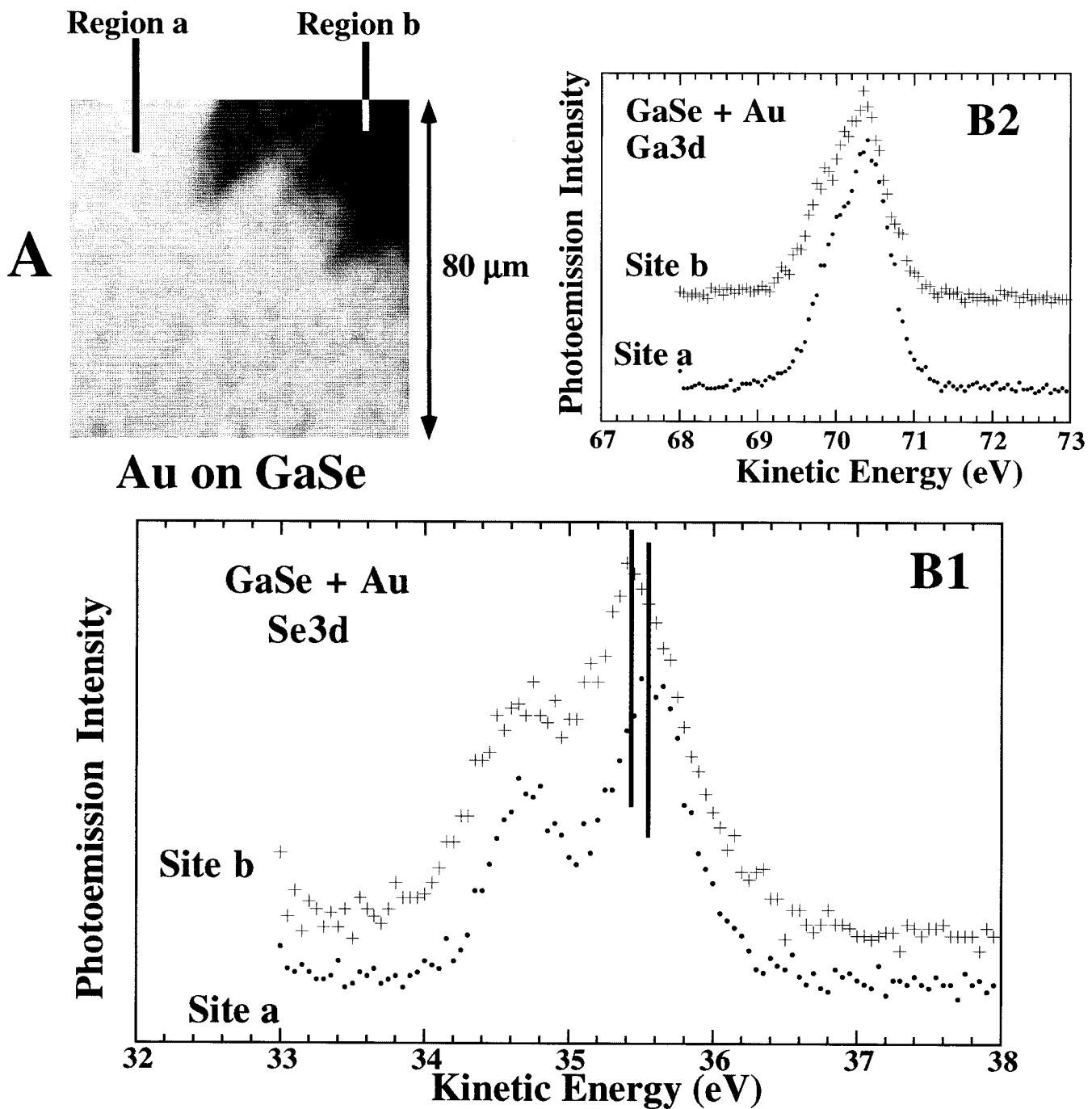


Figure 9. Scanning spectromicroscopy study of the fluctuations of the Schottky barrier over the interface between a (semiconducting) GaSe substrate and an Au overlayer [16]. (A) Micrograph, in which the contrast mechanism is linked to the barrier fluctuations which causes an electrostatic shift of the electron energies. (B1) and (B2) Core-level spectra from substrate elements from two different sample areas; note the rigid shifts of the peaks, indicating their electrostatic origin.

times more resolution than needed. This requires closing one or several slits in the photon monochromator systems, and/or their equivalent in the electron analyzer system—thereby decreasing the signal level at least by a factor of 10. To reach a sufficient signal level, you must increase the data accumulation time per spatial point (pixel): The overkill results in a waste of valuable time.

Note that you can overkill the lateral resolution as well as the energy resolution. Since there are two spatial coordinates, the effects could be dramatic. Combined overkills for the energy resolution and the spatial resolution is quite likely to lead to disaster.

Suppose, for example, that a micrograph of a given specimen reveals an interesting spatial feature, and that you want to learn

Cobalt in Granule Cells

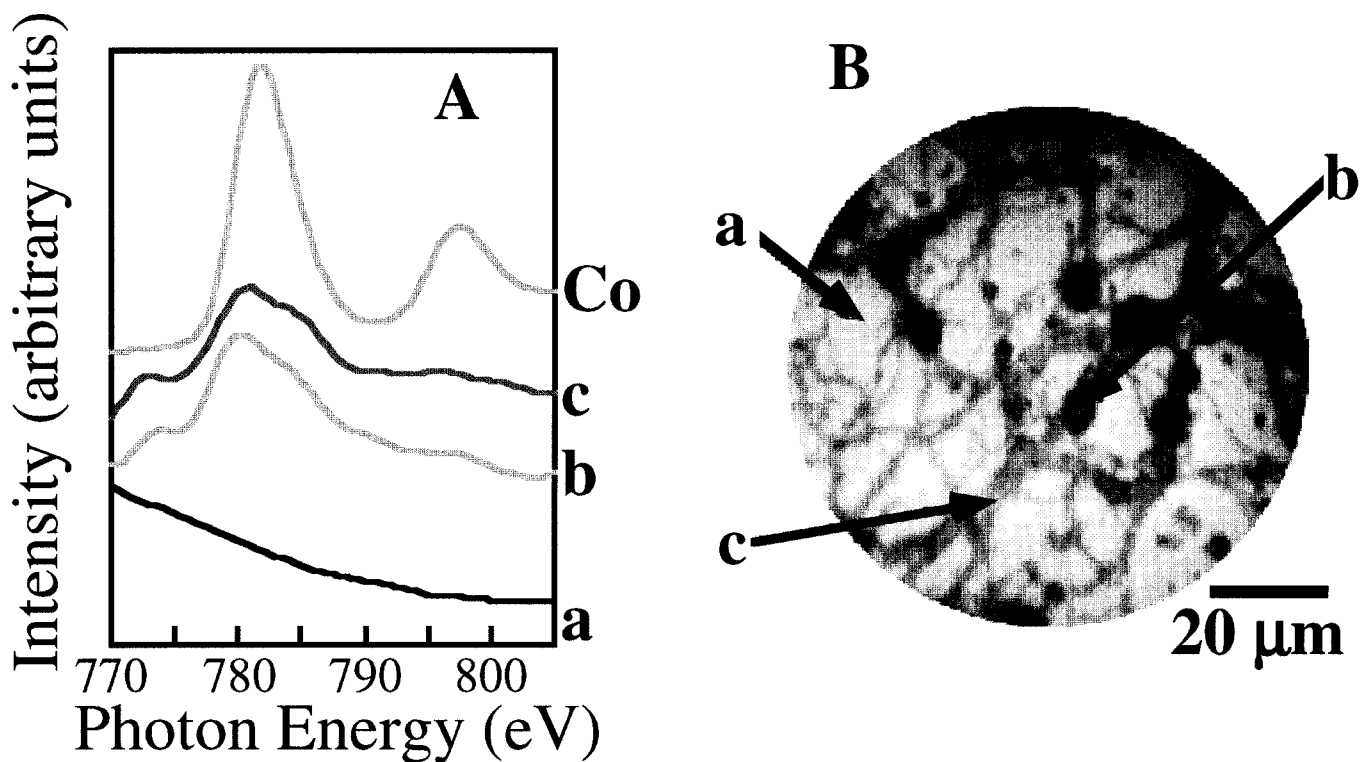


Figure 10. (A) X-ray absorption spectra taken with imaging photoelectron spectromicroscope XSEM in the two $10 \times 10\text{-}\mu\text{m}^2$ areas marked as (a), (b), and (c) in micrograph shown in (B), in the photon energy spectral range of the Co $L_{2,3}$ X-ray absorption edge. The top curve is the spectrum of a dried CoCl_2 droplet, curve a, which is from a substrate region does not show any Co-related signal. (B) Synchrotron photoelectron micrograph of a portion of a granule cell culture. The labels (a), (b), and (c) refer to the microscopic areas where the corresponding spectra of (A) were acquired. Data from G. F. Lorusso, G. De Stasio, D. Mercanti, M. Teresa Ciotti, D. Perret, A. Merbach, P. Perfetti, and G. Margaritondo, unpublished.

about the chemical properties of this feature; also suppose that the feature concerns only 5% of the 10^4 pixels of the micrograph. The correct strategy is to focus on the specific pixels of the feature, and to take complete spectra only from them, together with three to five reference spectra from the rest of the image.

Suppose instead that you adopt a brute-force approach, taking spectra from all pixels but then analyzing only those from the pixels of interest. You might justify the approach by arguing that one never knows what information might be required later. The cost of the wasted time, however, is so high that this “prudent” approach could be financially disastrous.

Suppose, in fact, that the data-taking time per spectrum is 1 min. The total time for the 5% pixels of the feature of interest is already more than 8 h. Without discrimination, the total time for 10^4 pixels is almost 170 h, of which more than 160 are potentially wasted. The equivalent beamtime cost at a synchrotron light facility can exceed \$80,000!

The problems of the data-taking strategy for spectromicroscopy are analyzed in detail in Ref. [9], using an information-entropy approach. These are the basic conclusions:

- The first general rule is that you must decide a priori what type of information you seek from the experiment, and develop a data-taking strategy to obtain that information and nothing else.
- Based on the sought information, the spatial and energy resolution levels must be selected to optimize the information content of the spectra. The “maximum extractable information” [9] from a spectrum or from an image is determined by the interplay of resolution and of the signal-to-noise level: Excessive resolution decreases the maximum extractable information because it negatively affects the signal-to-noise level. As a general rule [9], the maximum extractable information is optimized when the resolution is comparable to the size of the features that one must detect. For example, if in an image one tries to determine the position of a dot of diameter d , the spatial resolution which optimizes the image’s information content is also $\approx d$. Similarly, if one tries to measure the energy spectral position of a peak whose intrinsic width is δE , the optimum resolution is also $\approx \delta E$.

Carbon in Incinerated Granule Cells

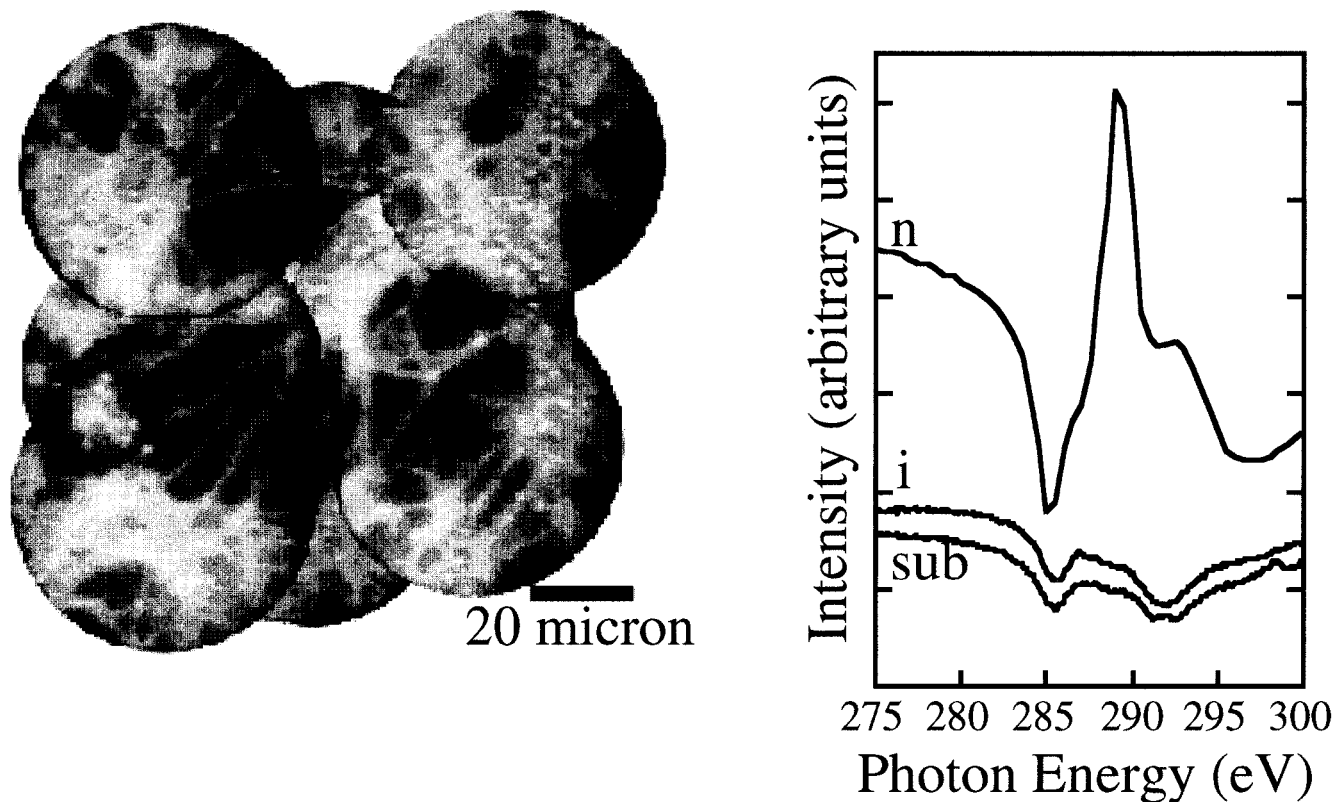


Figure 11. (A) Imaging photoelectron micrograph of a portion of an incinerated granule cell culture on a gold-coated silicon substrate. The image was obtained using the recently commissioned MEPHISTO microscope, illuminating the specimen with monochromatic photons of 140 eV. (B) X-ray absorption curves (raw data) in the C1s edge spectral region simultaneously taken on an incinerated cell structure (i curve) and on a substrate region (sub). The (n) curve shows similar data for a nonincinerated granule cell specimen. It is evident that carbon is removed by incineration. This conclusion is clear even if all spectra are affected by the carbon-related feature in the monochromator yield. The spot size from which data were taken was $10 \times 10 \mu\text{m}^2$.

- The data-taking strategy changes from one mode of spectromicroscopy to another; therefore, one cannot develop a general-purpose strategy. A specific analysis must be performed for each specific experiment [9].
- Errors in the data-taking strategy in spectromicroscopy cannot be compensated for by increasing the data-taking time, because of the high equivalent cost of the synchrotron light beamtime—which somebody must pay.
- Commonsense planning based on intuition can be helpful in some simple cases, but it could lead to an incorrect analysis in other cases, and to potential strategic disasters. Rigorous analysis [9] is always safer.

In a sense, therefore, spectromicroscopy with high-cost instruments forces the experimentalists to deal with engineering and cost-analysis problems that are not commonly found in conventional laboratory practice. The usual academic opinion that time and labor (graduate students) costs can be neglected clashes in this case with the reality of the high cost of centralized instruments such as synchrotron light sources.

On the positive side, improvements in the instrumentation—

most notably the photon sources—are producing an overall decrease in data-taking time. These are typical present performances: In the case of scanning spectromicroscopy with a Schwarzschild lens, a typical 100×100 -pixel image with $0.5 \mu\text{m}$ lateral resolution, which initially required several hours, can now be obtained in ≈ 30 min on a second-generation synchrotron source such as Aladdin in Wisconsin. This time should decrease by one order of magnitude on a third-generation source. A 100-point spectrum from one of the pixels with an energy resolution of 300–400 meV can be taken in several minutes, and this data taking should decrease to <1 min in the near future.

In the case of imaging spectromicroscopy, low-resolution (worse than $1 \mu\text{m}$) images can be taken in real time with a video system. Each submicron-resolution image requires an accumulation time on the order of 1 min. Therefore, this approach is faster than scanning spectromicroscopy, and this compensates its more limited spectroscopic capabilities. The image-taking times should again decrease by at least one order of magnitude with the advent of third-generation facilities. The data-taking time for a 100-point absorption spectrum (typical photon energy step of ≤ 20 –100 meV) is <1 min now and becoming shorter.

VI. SOME EXAMPLES OF APPLICATIONS

A. Scanning Spectromicroscopy. Figure 5 provided a good example of the analytical capabilities of techniques in this class. One should note, in addition, the domain of application which is peculiar to them and outside the realm of imaging spectromicroscopy: the study of local energy barriers.

Consider, for example, the interface between a semiconductor and a thin metal overlayer [32]. The charge configuration at the interface creates an extended dipole on the semiconductor side in the perpendicular direction. Such a dipole causes an energy barrier for free electric charge carriers such as free electrons or free holes. The barrier dominates the transport rectifying properties of this class of junctions and is called the Schottky barrier.

Schottky barriers are measured [15] with photoemission spectroscopy techniques, exploiting the fact that the barrier is electrostatic; therefore, the energies of all electronic states are equally affected by its presence—including the states from which photoelectrons originate. The photoelectron kinetic energy therefore will be influenced to some extent by the presence of the barrier, and can be used to measure it.

Experiments of this kind have been extensively performed for decades [15], but with a serious handicap: Because of the lateral-averaging character of photoemission spectroscopy, they could not detect local fluctuations in the barrier height. In turn, these fluctuations are quite important both from a fundamental point of view and in practical applications. The handicap was removed [16] by the advent of scanning photoelectron spectromicroscopy.

Consider Figure 9, which shows [16] a photoelectron micrograph of the interface between a GaSe (semiconducting) substrate and an Au overlayer: The intensity fluctuations are due to neither chemical differences nor geometric differences, but to a third factor: the fluctuations in the electrostatic contribution to the electron energies by the Schottky barrier.

This point is elucidated by Figure 9(B), which shows core-level spectra from the two components of the substrate. The energy shifts from point to point are equal for the two spectra, suggesting an electrostatic rather than chemical difference—indeed, the electrostatic difference due to fluctuations of the Schottky barrier from point to point.

Similar experiments have been performed in recent years for different types of interface energy barriers: not only Schottky barriers, but also those at semiconductor–semiconductor interfaces [17] and at the interface between semiconductors or insulators and vacuum [33]. The results are revolutionizing our picture of interface energy barriers, revealing in many cases substantial fluctuations and stimulating a more extensive use of scanning spectromicroscopy in this domain.

B. Imaging Spectromicroscopy. Biological applications are a prime domain for this class of techniques, and the most extensive experiments have been performed on brain cell specimens [2]. For example, the uptake of cobalt by brain cell cultures is being extensively investigated [34] because of its importance in understanding several Co^{2+} -related physiological mechanisms such as neuron membrane polarization [35,36].

Cobalt accumulation is well known to occur in granule cells in the presence of excitatory amino acids such as kainate [35,36]. We obtained with the XSEM data of Figure 10 evidence of cobalt in granule cells in the absence of kainate (G. F. Lorusso, G. De Stasio, D. Mercanti, M. Teresa Ciotti, D. Perret, A. Merbach,

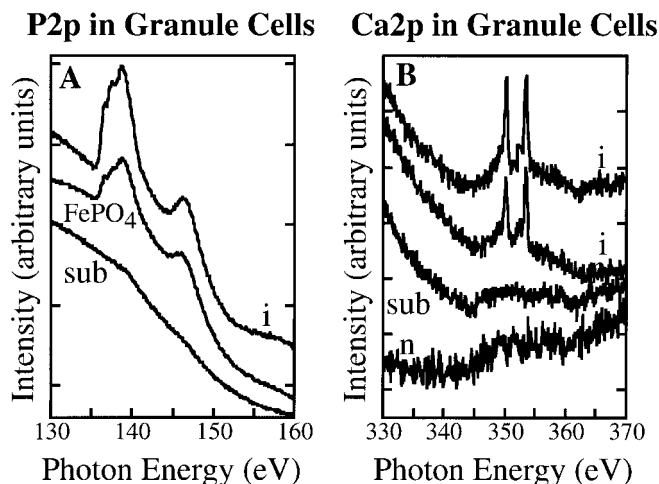


Figure 12. X-ray absorption curves in the P2p (A) and Ca2p (B) edge spectral regions simultaneously taken on cell structures (i) and on substrate regions (sub) of an incinerated granule cell specimen similar to the one shown in Figure 11(A). (n) Similar data for nonincinerated granule cell specimens. Also shown is a reference spectrum taken on a dried droplet of FePO_4 in water. It is clear that the relative calcium content is strongly enhanced by incineration.

P. Perfetti, and G. Margaritondo, unpublished). The cells were exposed to a 5-mM solution of CoCl_2 in buffer in the absence of excitatory amino acids, and then carefully washed to remove all the nonuptaken cobalt. In Figure 10, we see X-ray absorption spectra taken in the spectral region of the Co $L_{2,3}$ edge in different microscopic areas (approximate size: $10 \times 10 \mu\text{m}^2$) of the granule cell culture. The spectra were taken in the correspondingly labeled areas of the photoelectron micrograph of the same figure, and they clearly show the presence of Co, even though no excitatory amino acid was used.

This is precisely the result that our present data demonstrate. We find cobalt where other histochemical techniques failed to detect it, arguably because of the higher sensitivity of our spectromicroscopic approach to this problem.

As already mentioned, the incineration technique can be used to enhance the concentration of certain elements present in biological samples, removing carbon, nitrogen, and hydrogen [31]. In Figure 11(A), we present a micrograph, obtained with MEPHISTO, of a portion of an incinerated granule cell culture. From the spectra reported in Figure 11(B) it is evident that carbon is removed by the incineration process (the C1s peaks disappear), while in the spectra of Figure 12 it is clear that phosphorus and calcium peaks are more intense, and therefore their concentration is increased.

Many chemical elements can play an important role in brain cell physiology and pathology, and the number of scanning spectromicroscopy experiments in this domain is rapidly expanding. We will briefly discuss experiments on zinc [36], which give us the opportunity to illustrate how surface sensitivity can in some cases become an advantage rather than a disadvantage.

Usually, the surface sensitivity of spectromicroscopy is considered a handicap (see the above discussion of possible remedies). In the study of the microchemical distribution of zinc, it turned out to be a positive factor, because it allowed us to discrim-

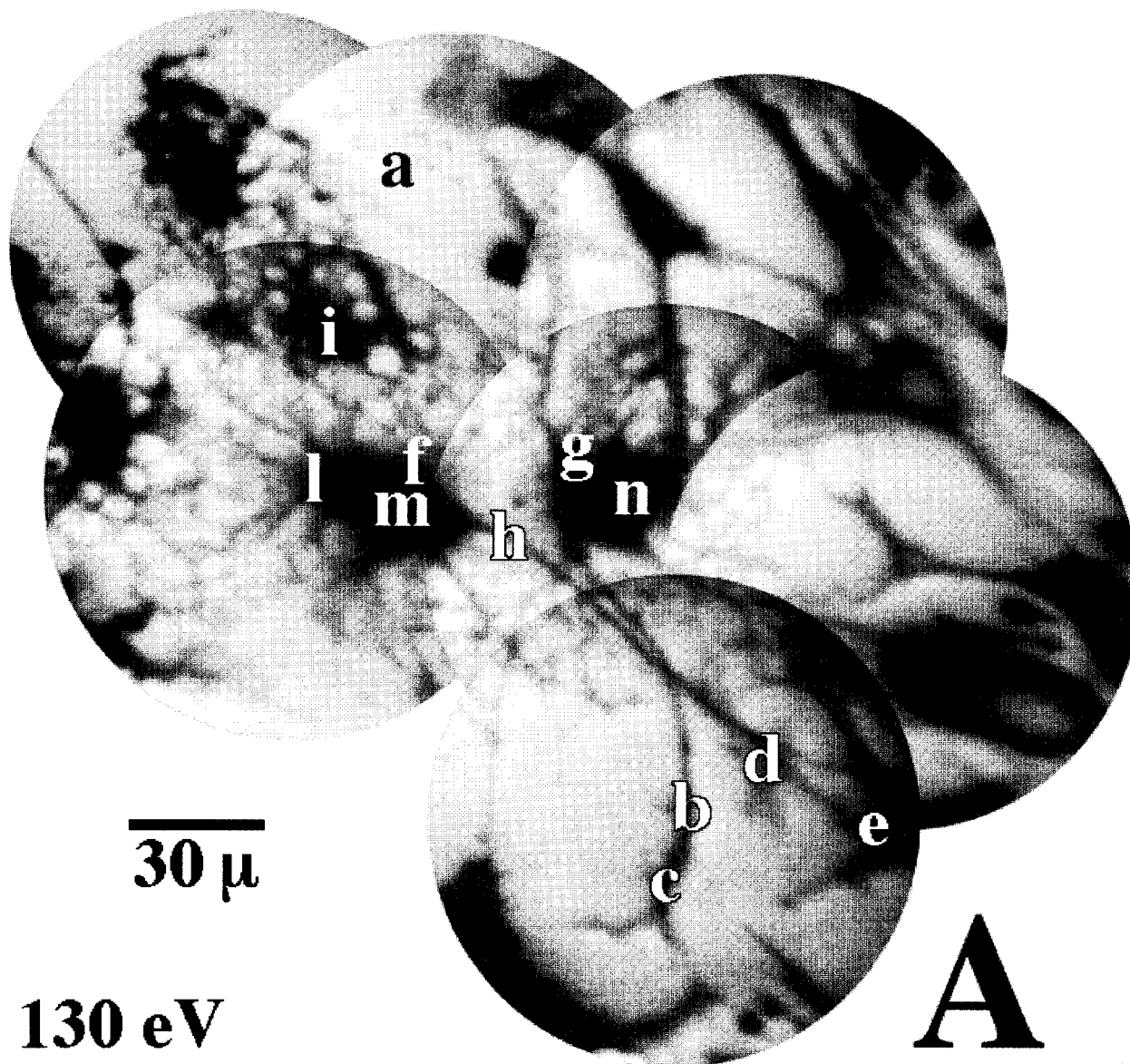


Figure 13. (A) Combination of XSEM micrographs of astrocytes, found as a subpopulation of a culture with prevailing glial cells, after exposure to a 5 mM ZnCl_2 solution for 20 min. The photon energy was 130 eV. The letters identify the microscopic ($\sim 3 \times 3 \mu\text{m}^2$) regions in which the spectra of Figure 10(B) were taken. (B) XSEM (X-ray absorption) spectra from these regions. The data were background-corrected, normalized and twice-smoothed over five-point sets. Curve (a) refers to a substrate area and is the only one not showing the typical Zn3s absorption threshold lineshape. Curve (o) is a reference spectrum from a dried droplet of a zinc sulfate solution. Data from Ref. 36.

inate zinc uptake in the “surface” (the membrane) of cells, and their “bulk” (the cytoplasm).

The uptake of zinc by cerebellar rat cultures upon exposure to ZnCl_2 solutions was investigated with two different techniques: imaging spectromicroscopy with the XSEM and inductively-coupled-plasma atomic emission spectroscopy (ICP-AES) [37]. The ICP-AES results clearly demonstrate that the exposure significantly enhances the bulk Zn concentration with respect to the physiological level, whereas imaging spectromicroscopy revealed that the effect on the surface (cell membrane) is negligible.

We observed zinc in a variety of different cell types, including glial cell granules and Purkinje neurons and oligodendrocytes,

all exposed to zinc solutions for variable periods of time, and variable exposure solution zinc concentrations. Figure 13 shows an example of the spectromicroscopy results obtained on oligodendrocytes.

Using imaging spectromicroscopy, we did not observe significant differences in the zinc content between the different cells, different times of exposure, or concentrations. Thus, the amount of physiologically present zinc in the region probed by imaging spectromicroscopy (the surface) is not altered by the exposure process: The amount of zinc present with or without exposure to a zinc solution was quite similar.

Parallel experiments performed with ICP-AES, on the other

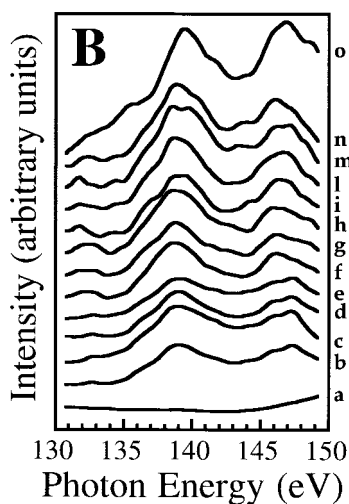


Figure 13. Continued

hand, clearly demonstrated a time dependence and a concentration dependence in the zinc uptake increase after the exposure of cell cultures to zinc solutions. Thus, the effect of exposure is primarily a bulk phenomenon. The main difference between spectromicroscopy and ICP-AES, in fact, is surface sensitivity. In imaging spectromicroscopy, one probes the first 100–200 Å of the sample surface. In the case of cells, therefore, the probed depth includes the cell membrane (50 Å thick), part of the membrane proteins, and only a small portion of the cytoplasm.

The physiological presence of Zn, independent of any exposure, both in the membrane and in the cytoplasm, is not surprising: for example, in light of the existence of Zn-binding proteins. The differences between imaging spectromicroscopy and ICP-AES data, on the other hand, indicate that the artificial Zn exposures significantly increase only the Zn content in the cytoplasm. This could be either due to a large physiological amount of Zn in the membrane, which is only marginally affected by the exposures, or to a more effective mechanism for exposure-caused uptake in the cytoplasm—or else, to a combination of both effects. The present results cannot definitely rule out any one of these effects. Speculatively, one tends to favor the first conjecture, because of the hypothesized involvement of Zn in synaptic transmission [38].

VII. FUTURE DIRECTIONS

The few examples discussed in our review clearly show that photoelectron spectromicroscopy is no longer a technique under feasibility testing, but a mature probe used for real and systematic experiments. We expect this trend to accelerate in the future as the capabilities of these novel experiments become better known, notably to the life-science community.

On the other hand, this entire field is being boosted by the exceptional improvements in the quality of synchrotron light sources. The mid-1980s brought the transition from the second to the third generation of sources [5]. This implied a shift in emphasis from the flux of the source to brightness [5,8], that is, to the combination of high flux, small source size, and small

angular divergence. Brighter sources are much easier to focus than low-brightness sources; hence, the strong impact of the third-generation synchrotrons on microscopy and spectromicroscopy [5,8].

Techniques in this domain, in fact, play a leading role both at the ALS and at Elettra [13,39], and are emerging as leaders also at the other third-generation soft-X-ray facilities in Pohang, Korea, Hsinchu, Taiwan [40], and Lund, Sweden. We can already foresee a fourth generation of sources. The Swiss light source (SLS) [13] proposed by the Paul-Scherrer Institut in Villigen is designed to increase the brightness by at least a factor of five. The impact on microscopy and spectromicroscopy is quite obvious.

Furthermore, the increase in brightness, primarily due to improved geometric factors, also implies another important development: The new sources are becoming very highly coherent. One can distinguish between two kinds of coherence: longitudinal and lateral. Longitudinal coherence depends on the spectral bandwidth of the source; high brightness enhances the effectiveness of monochromators in decreasing the bandpass while keeping a high flux, thus allowing high longitudinal coherence. Lateral coherence depends on the source size and angular divergence. Thus, high brightness caused by low source size and low divergence also means high lateral coherence.

Elettra already reaches almost complete coherence for photon energies up to 10 eV and substantial coherence up to 1–10 keV. With the SLS, the full-coherence limit would be pushed up to 100 eV or more. This means that coherence-based techniques are already feasible, notably holography. One could envision, therefore, an exciting expansion of microscopy and spectromicroscopy in the direction of atomic-level holography.

ACKNOWLEDGMENTS

The authors' own research in spectromicroscopy is performed in cooperation with the authors of Refs. 2, 11, 13, 18–20, 23–25, 29, 32, 33, 36, 37, and 41.

REFERENCES

1. G. Margaritondo and F. Cerrina. "Overview of soft-x-ray photoemission spectromicroscopy," *Nucl. Instr. Methods* **A291**, 26 (1990).
2. G. De Stasio, F. Cerrina, B. P. Tonner, D. Mercanti, and G. Margaritondo. "Spectromicroscopy in biophysics," *Life Chem. Rep.* **11**, 79 (1994).
3. G. Margaritondo, "X-ray microscopy and holography", in *From Galileo's 'Occhialino' to Optoelectronics*. Paolo Mazzoldi, Ed., World Scientific, Singapore 1993, p. 161 and references therein.
4. G. Margaritondo. "Photoemission and free electron laser spectromicroscopy: Photoemission at high lateral resolution," *Scann. Spectromicrosc.* **9**, 949 (1995).
5. G. Margaritondo. "Synchrotron light and free electron lasers," *Riv. Nuovo Cimento* **18**, 1 (1995).
6. G. Margaritondo, J. Almeida, and Gelsomina De Stasio, "Recent progress in synchrotron radiation spectroscopy and spectromicroscopy," *J. Jap. Soc. Synchr. Radiat. Res.* **8**, 521 (1995).
7. G. Margaritondo. "100 years of photoemission," *Phys. Today* **41**, 66 (1988).
8. G. Margaritondo. "A primer in synchrotron radiation: Everything you wanted to know about SEX (synchrotron emission of x-rays) but were afraid to ask," *J. Synchr. Rad.* **2**, 148 (1995).
9. G. Margaritondo. "The information content of photoemission spectroscopy and spectromicroscopy," *Surf. Rev. Lett.* **2**, 305 (1995).

10. B. P. Tonner and D. Dunham. "Submicron spatial resolution of a micro-EXAFS electrostatic microscope with bending magnet radiation: Performance assessments and prospects for aberration correction," *Nucl. Instrum. Methods* **A347**, 436 (1994) and references therein.
11. B. P. Tonner, G. R. Harp, S. F. Koranda, and J. Zhang. "An electrostatic microscope for synchrotron radiation x-ray absorption microspectroscopy," *Rev. Sci. Instrum.* **63**, 564 (1992).
12. G. De Stasio, G. F. Lorusso, T. Droubay, M. Kohli, P. Murali, P. Perfetti, G. Margaritondo, T. F. Kelly, and B. P. Tonner. "An electron imaging approach to soft-x-ray transmission spectromicroscopy," *Rev. Sci. Instrum.* **67**, 737 (1996).
13. H. J. Weyer and G. Margaritondo. "Towards the next generation: the Swiss light source," *Synchr. Radiat. News* **8**, 19 (1995).
14. W. Gudat and C. Kunz. "Close similarity between photoelectric yield and photoabsorption spectra in the soft-x-ray range," *Phys. Rev. Lett.* **29**, 169 (1972).
15. G. Margaritondo, *Introduction to Synchrotron Radiation* (Oxford University Press, New York), 1988.
16. F. Gozzo, M. Marsi, H. Berger, G. Margaritondo, A. Ottolenghi, A. K. Ray-Chaudhuri, W. Ng, S. Liang, S. Singh, J. T. Welnak, J. P. Wallace, C. Capasso, and F. Cerrina. "Microscopic-scale lateral inhomogeneities of the Schottky Barrier formation process," *Phys. Rev.* **B48**, 17163 (1993).
17. F. Gozzo, H. Berger, I. R. Collins, G. Margaritondo, W. Ng, A. K. Ray-Chaudhuri, S. Liang, S. Singh, and F. Cerrina. "Microscopic-scale lateral inhomogeneities of the GaSe-Ge heterojunction energy lineup," *Phys. Rev.* **B51**, 5024 (1995).
18. W. Ng, A. K. Ray-Chaudhuri, S. Liang, S. Singh, H. Solak, J. Welnak, F. Cerrina, G. Margaritondo, J. H. Underwood, J. B. Kortright, and R. C. C. Perera. "High resolution spectromicroscopy with MAXIMUM: Photoemission spectroscopy reaches the 1000 E scale," *Nucl. Instrum. Methods* **A347**, 422 (1994), and references therein.
19. C. Capasso, W. Ng, A. K. Ray-Chaudhuri, S. H. Liang, R. K. Cole, Z. Y. Guo, J. Wallace, F. Cerrina, J. Underwood, R. Perera, J. Kortright, G. De Stasio, and G. Margaritondo. "Scanning photoemission spectromicroscopy on MAXIMUM reaches 0.1 micron resolution," *Surf. Sci.* **287/88**, 1046 (1993), and references therein.
20. J. Kirz, H. Ade, E. Anderson, C. Buckley, H. Chapman, M. Howells, C. Jacobsen, C. H. Ko, S. Lindaas, D. Sayre, S. Williams, S. Wirick, and X. Zhang. "New results in soft-x-ray microscopy," *Nucl. Instrum. Methods* **B87**, 92 (1994), and references therein.
21. J. Kirz, H. Ade, C. Jacobsen, C. H. Ko, S. Lindaas, I. McNulty, D. Sayre, S. Williams, S. Wirick, and X. Zhang. "Soft-x-ray microscopy with coherent x-rays," *Rev. Sci. Instrum.* **63**, 557 (1992), and references therein.
22. J. Welnak, Z. Dong, H. Solak, J. Wallace, F. Cerrina, M. Bertolo, A. Bianco, S. Di Fonzo, S. Fontana, W. Jark, F. Mazzolini, R. Rosei, A. Savoia, J. H. Underwood, and G. Margaritondo. "SUPERMAXIMUM: A Schwarzschild-based spectromicroscope for ELETTRA," *Rev. Sci. Instrum.* (in press).
23. F. Cerrina, B. Lai, C. Gong, A. Ray-Chaudhuri, G. Margaritondo, M. A. Green, H. Höchst, R. Cole, D. Crossley, S. Collier, J. Underwood, L. J. Brillson, and A. Franciosi. "MAXIMUM: Status of the scanning photoelectron microscope," *Rev. Sci. Instrum.* **60**, 2249 (1989).
24. G. De Stasio, W. Ng, A. K. Ray-Chaudhuri, R. K. Cole, Z. Y. Guo, J. Wallace, G. Margaritondo, F. Cerrina, J. Underwood, R. Perera, J. Kortright, Delio Mercanti, and M. Teresa Ciotti. "Scanning photoelectron microscopy with undulator radiation: a successful test on uncoated neurons," *Nucl. Instrum. Methods* **A294**, 351 (1990).
25. G. Margaritondo, A. Savoia, S. Bernstoff, M. Bertolo, G. Comelli, F. De Bona, W. Jark, M. Kiskinova, G. Paolucci, K. C. Prince, A. Santaniello, G. Tromba, R. Walker, and R. Rosei. "The ultrabright synchrotron source ELETTRA: First period of operation," *Acta Phys. Polonica* (in press).
26. G. Comelli, M. Kiskinova, G. Paolucci, K. C. Prince, A. Savoia, and G. Margaritondo. "Photoemission latest news: Time resolution, microanalysis, order parameters," *Surf. Rev. Lett.* (in press).
27. L. Y. Huang. "Rvntgen-Bildwandler-mikroskopie," *Z. Phys.* **149**, 225 (1957).
28. F. Polack and S. Lowenthal. "Photoelectron microscope for x-ray microscopy and microanalysis," *Rev. Sci. Instrum.* **52**, 207 (1981).
29. F. Polack and S. Lowenthal. "Project of a photoelectron x-ray microscope on ACO storage ring," *Nucl. Instrum. Methods* **208**, 373 (1983).
30. G. De Stasio, A. Cricenti, R. Generosi, D. Mercanti, M. T. Ciotti, P. Casalbore, G. Margaritondo, and P. Perfetti. "Neurone decapping characterization by atomic force microscopy," *Neuroreports* (in press).
31. M.-J. Davicco, V. Coxam, N. Gaumet, P. Lebecque, and J. P. Barlet. "Eb-1089, a calcitriol analog, decreases fetal calcium content when injected into pregnant rats," *Exp. Physiol.* **80**, 449 (1995).
32. L. J. Brillson, Ed., *Contacts to Semiconductors* (Noyes, Mill Road, NJ), 1993.
33. F. Cerrina, A. K. Ray-Chaudhuri, W. Ng, S. Liang, S. Singh, J. T. Welnak, J. P. Wallace, C. Capasso, J. H. Underwood, J. B. Kortright, R. C. C. Perera, and G. Margaritondo. "Microscopic-scale lateral inhomogeneities of the photoemission response of cleaved GaAs," *Appl. Phys. Lett.* **63**, 63 (1993).
34. G. De Stasio, D. Mercanti, M. Teresa Ciotti, T. C. Droubay, P. Perfetti, G. Margaritondo, and B. P. Tonner. "Synchrotron spectromicroscopy of cobalt accumulation in granule cells, glial cells and GABAergic neurons," *J. Phys.* **D29**, 259 (1996).
35. R. M. Pruss, R. L. Akesson, M. M. Racke, et al. "Agonist-activated cobalt uptake identifies divalent-cation permeable kainate receptors on neurons and glial-cells," *Neuron* **7**, 509 (1991).
36. S. J. Butke, H. Yin, and J. H. Weiss. "Ca²⁺ and in-vitro kainate damage to cortical and hippocampal Smi-32(+) neurons," *Neuroreport* **6**, 629 (1995).
37. G. De Stasio, S. Pochon, G. F. Lorusso, B. P. Tonner, D. Mercanti, M. Teresa Ciotti, N. Oddo, P. Galli, P. Perfetti, and G. Margaritondo. "Zinc uptake by brain cells: Surface vs. bulk," *J. Phys. D* (in press).
38. A. Varma, *Handbook of Inductively Coupled Plasma Atomic Emission Spectroscopy* (CRC, Boca Raton, FL), 1991, p. 380.
39. J. Koh and D. W. Choi. "Zinc excitatory amino-acids neurotoxicity on cortical-neurons," *J. Neurosci.* **8**, 2164 (1988).
40. A. Abrami, D. Alfè, S. Antonini, M. Bernardini, M. Bertolo, C. J. Bocchetta, D. Bulfone, F. Cargnello, F. Daclon, S. Di Fonzo, S. Fontana, A. Galimberti, M. Giannini, W. Jark, A. Massarotti, F. Mazzolini, M. Puglisi, R. Richter, A. Rindi, R. Rosei, C. Rubbia, D. Tommasini, A. Savoia, G. Viani, R. P. Walker, A. Wrulich, C. Coluzza, T. dell'Orto, F. Gozzo, G. Margaritondo, G. De Stasio, P. Perfetti, M. Gentili, M. T. Ciotti, and D. Mercanti. "First experimental tests at the new synchrotron radiation facility ELETTRA in Trieste," *Nucl. Instrum. Methods* **A349**, 609 (1994).
41. Y. Hwu, C. Y. Tung, C. Y. Pieh, S. D. Lee, P. Alméras, F. Gozzo, H. Berger, G. Margaritondo, G. De Stasio, D. Mercanti, and M. Teresa Ciotti. "First spectromicroscopy tests at the Taiwan Synchrotron Radiation Research Center (SRRC): Chemical and topographic microimaging of layered systems," *Nucl. Instrum. Methods* **A361**, 349 (1995).